



Supplement of

A quantitative method of resolving annual precipitation for the past millennia from Tibetan ice cores

Wangbin Zhang et al.

Correspondence to: Shugui Hou (shugui@nju.edu.cn, shuguihou@sjtu.edu.cn)

The copyright of individual parts of the supplement might differ from the article licence.

10 **Text S1**

In this study, the depth-age relationship of the Chongce 135.81 m Core 2 was established by using a two-parameter (2p) model. The 2p model was first constrained by the ^{14}C calibrated ages, together with the β -activity reference horizon of the Chongce 58.82 m Core 3, located only ~ 2 meters apart (Hou et al., 2018; Pang et al., 2020). We found that by using these data only, the 2p model is poorly constrained at the deep section, and giving an estimate bottom age much older than the bottom age ($8.3 \pm \frac{6.2}{3.6}$ ka B.P.) estimated for Core 4 (Hou et al., 2018). Therefore, we included the Core 4 bottom age to constrain the final 2p model. Due to its mathematical configuration to account for ice flow dynamics, the 2p model gives more weight to points at shallower sections. Therefore, the inclusion of the Core 4 bottom age (relatively younger than otherwise derived bottom age) pushes the curve towards the left (younger) of most ^{14}C dates. However, we believe this model gives the most reasonable results, compared with several other model fit based on different data combinations (Fig. S7). The details of these model fits are provided as follows.

(1) all data (including β -activity peak of Core 3 and nine ^{14}C ages) (Fig. S7a).

Results: The derived annual accumulation rate of 137 ± 54 mm w.e./year is in good agreement with the value of 140 mm w.e./year based on the tritium horizon. But the model is poorly constrained in deeper sections: the derived age estimate at the depth of the deepest ^{14}C sample is $9.1 \pm \frac{7.2}{4.0}$ ka B.P.. This is much older than the actual measured ^{14}C age of 6.3 ± 0.2 ka B.P. at that depth (Fig. S7a).

(2) all data (including β -activity peak of Core 3 and nine ^{14}C ages) and constant accumulation rate (140 m w.e./year) (Fig. S7b).

Results: The derived ice age at the bedrock is $30.7 \pm \frac{44.8}{18.4}$ ka B.P., which is much older than the bottom age ($8.3 \pm \frac{6.2}{3.6}$ ka B.P.) estimated for Core 4. In addition, the derived age estimate at the depth of the deepest ^{14}C sample is $9.2 \pm \frac{6.0}{3.6}$ ka B.P.. This is much older than the ^{14}C age of 6.3 ± 0.2 ka B.P. at that depth. (Fig. S7b).

(3) β -activity peak of Core 3 and oldest six ^{14}C ages (Fig. S7c).

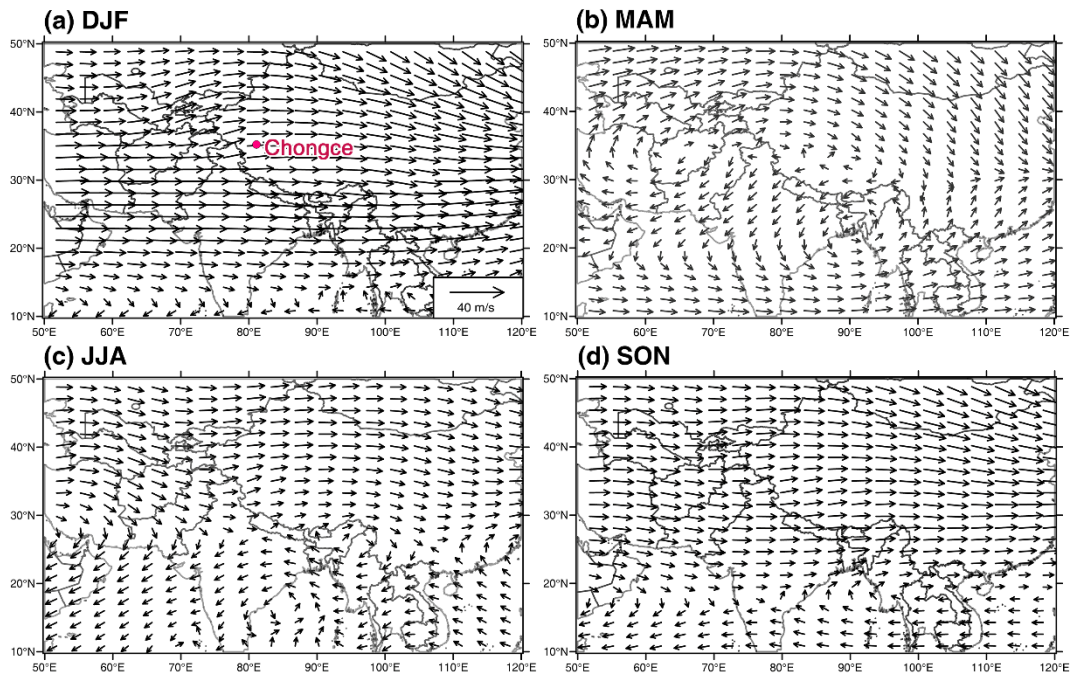
Results: The derived ice age at the bedrock is $22.5 \pm \frac{34.8}{13.8}$ ka B.P., which is much older than the bottom age ($8.3 \pm \frac{6.2}{3.6}$ ka B.P.) estimated for Core 4. In addition, the derived accumulation (233 ± 104 mm w.e./year) deviates significantly from the β -activity based estimate (140 mm w.e./year) (Fig. S7c).

(4) β -activity peak of Core 3, oldest six ^{14}C ages, and constant accumulation rate (140 mm w.e./year) (Fig. S7d).

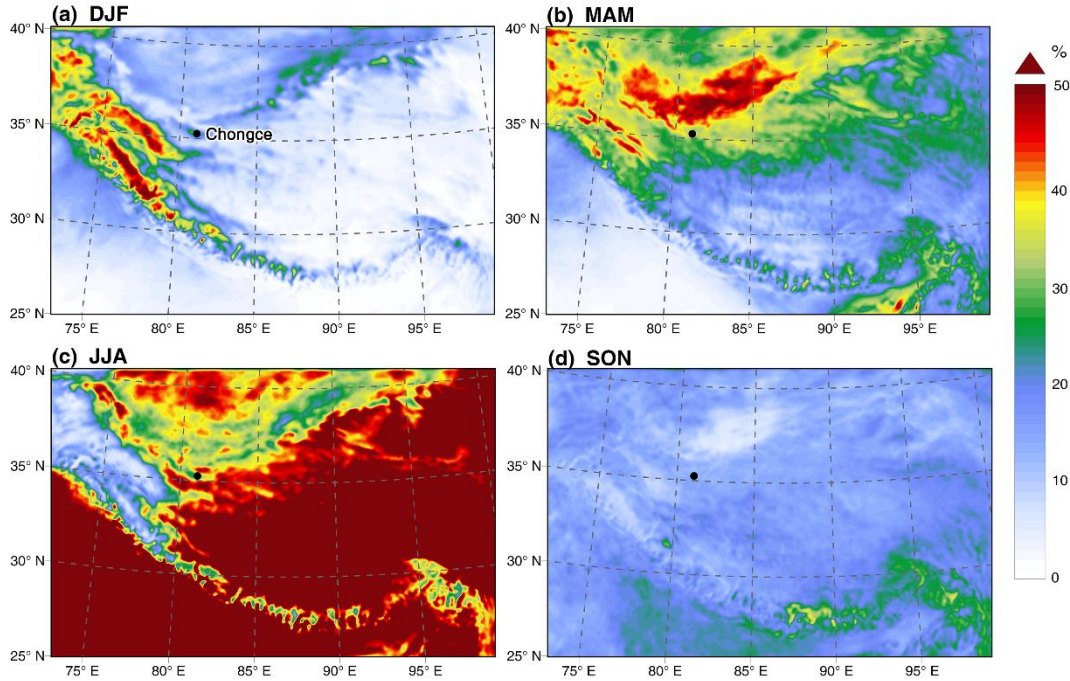
40 Results: The derived ice age at the bedrock is $50.1 \pm \frac{118.4}{35.6}$ ka B.P., which is much older than the bottom age ($8.3 \pm \frac{6.2}{3.6}$ ka B.P.) estimated for Core 4. In addition, the derived age estimate at the depth of the deepest ^{14}C sample is $9.6 \pm \frac{7.3}{4.1}$ ka B.P.. This is much older than the ^{14}C age of 6.3 ± 0.2 ka B.P. at that depth (Fig. S7d).

(5) all data (including β -activity peak of Core 3 and nine ^{14}C ages) plus bedrock estimate from Core
45 4 (Hou et al., 2018) as an additional model input point (**the method used in this manuscript**) (Fig. S7e).

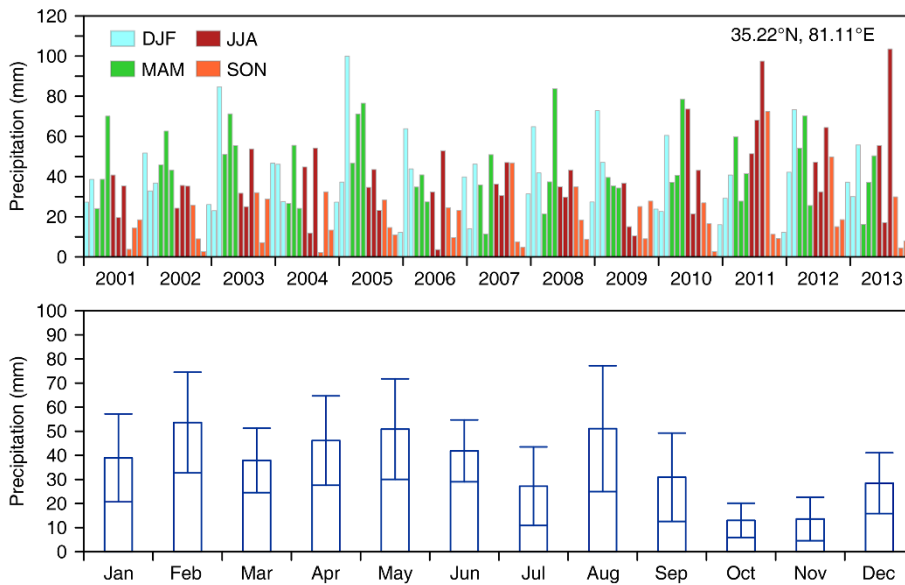
Results: The derived ice age at the bedrock is $9.0 \pm \frac{7.9}{3.6}$ ka B.P., which is roughly consistent with the bottom age ($8.3 \pm \frac{6.2}{3.6}$ ka B.P.) estimated for Core 4. The derived accumulation rate (103 ± 34 mm w.e./year) is in relative agreement with the β -activity based estimate (140 mm w.e./year). In addition, the modeled age at the depth of the deepest ^{14}C sample is now $5.2 \pm \frac{1.9}{1.2}$ ka B.P. which, with the uncertainty
50 range, is similar to the ^{14}C age of 6.3 ± 0.2 ka B.P. (Fig. S7e). We believe this model provides most reasonable results, and is therefore adopted for this paper.



55 **Figure S1.** Seasonally averaged horizontal wind patterns at 500 hPa over the Tibetan Plateau and its vicinity. Wind speed data are from the ERA 5 (available at: <https://www.ecmwf.int/>).



60 **Figure S2.** Seasonal precipitation regimes on the Tibetan Plateau. Percentage of annual precipitation in winter (DJF) (a), spring (MAM) (b), summer (JJA) (c), and fall (SON) (d), calculated by the High Asia Refined analysis dataset (2001-2013 AD) with spatial resolution of 10 km (Maussion et al., 2014).



65 **Figure S3.** Monthly precipitation distribution in the vicinity of the Chongce ice cap, as shown by High Asia Refined monthly data from 2001 A.D. to 2013 A.D. (top) and by the monthly climatology for this period (bottom) (Maussion et al., 2014). Approximately 27.8% of annual precipitation falls from June to August, 13.3% from September to November, 27.9% from December to February, and 31.1% from

March to May.

70

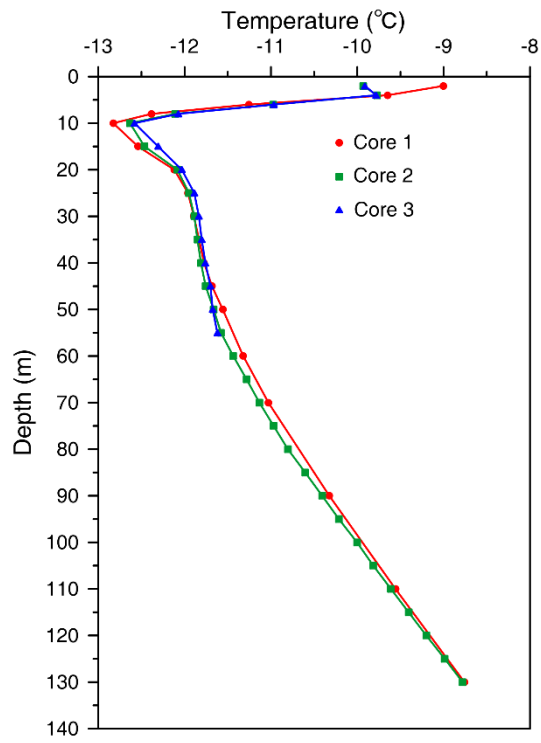
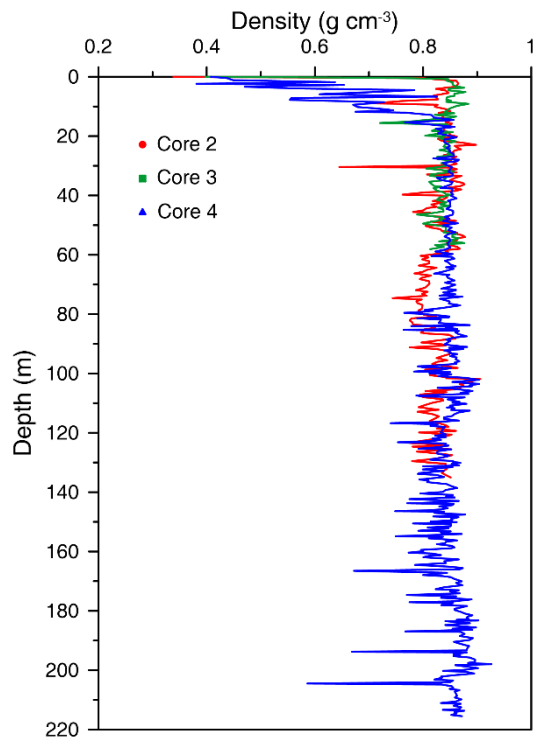


Figure S4: Borehole temperature profiles of the Chongce Core 1, Core 2 and Core 3



75

Figure S5. Density profiles of the Chongce Core 2, Core 3 and Core 4.

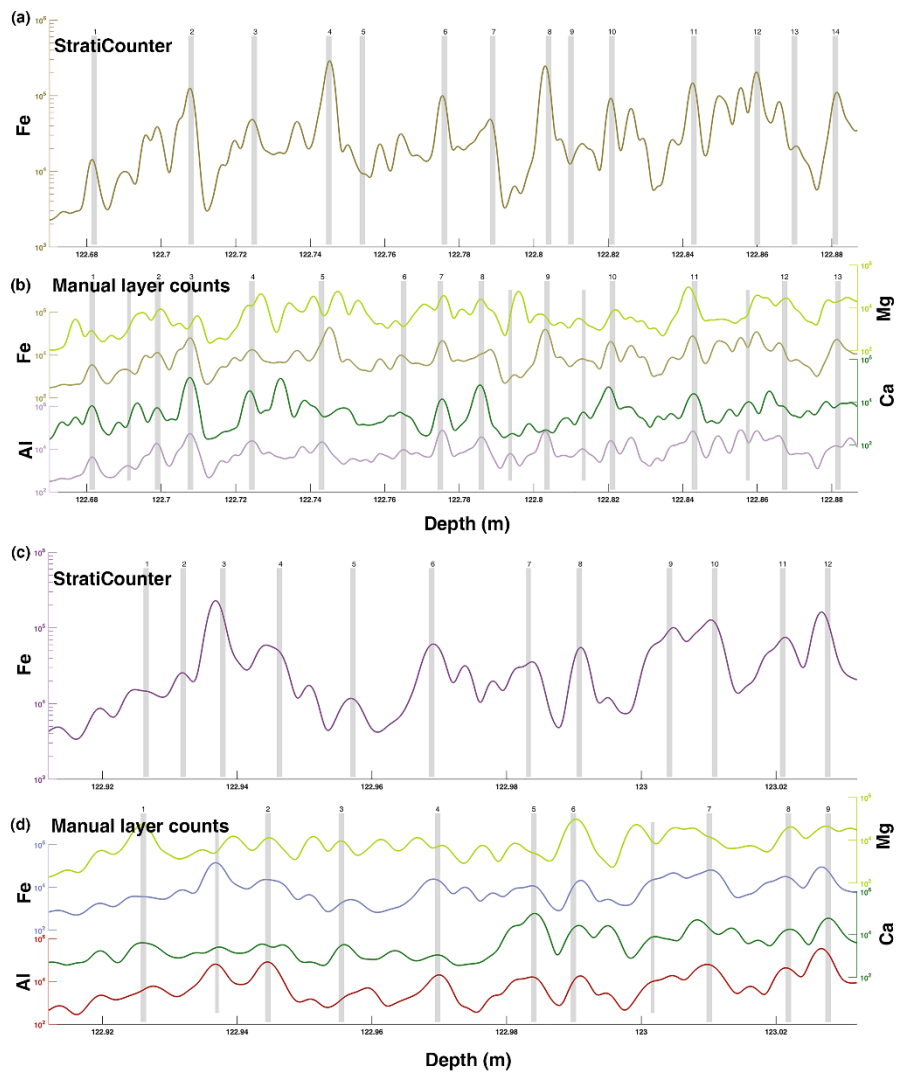


Figure S6. StratiCounter assignment of annual layers for Section III (a, c). Manual assignment of annual layers for Section III (b, d). The annual layers of Section III are marked at the winter/spring peaks (grey bars) of Al, Ca, Fe, and Mg concentrations. The short grey bars indicate uncertain annual layers.

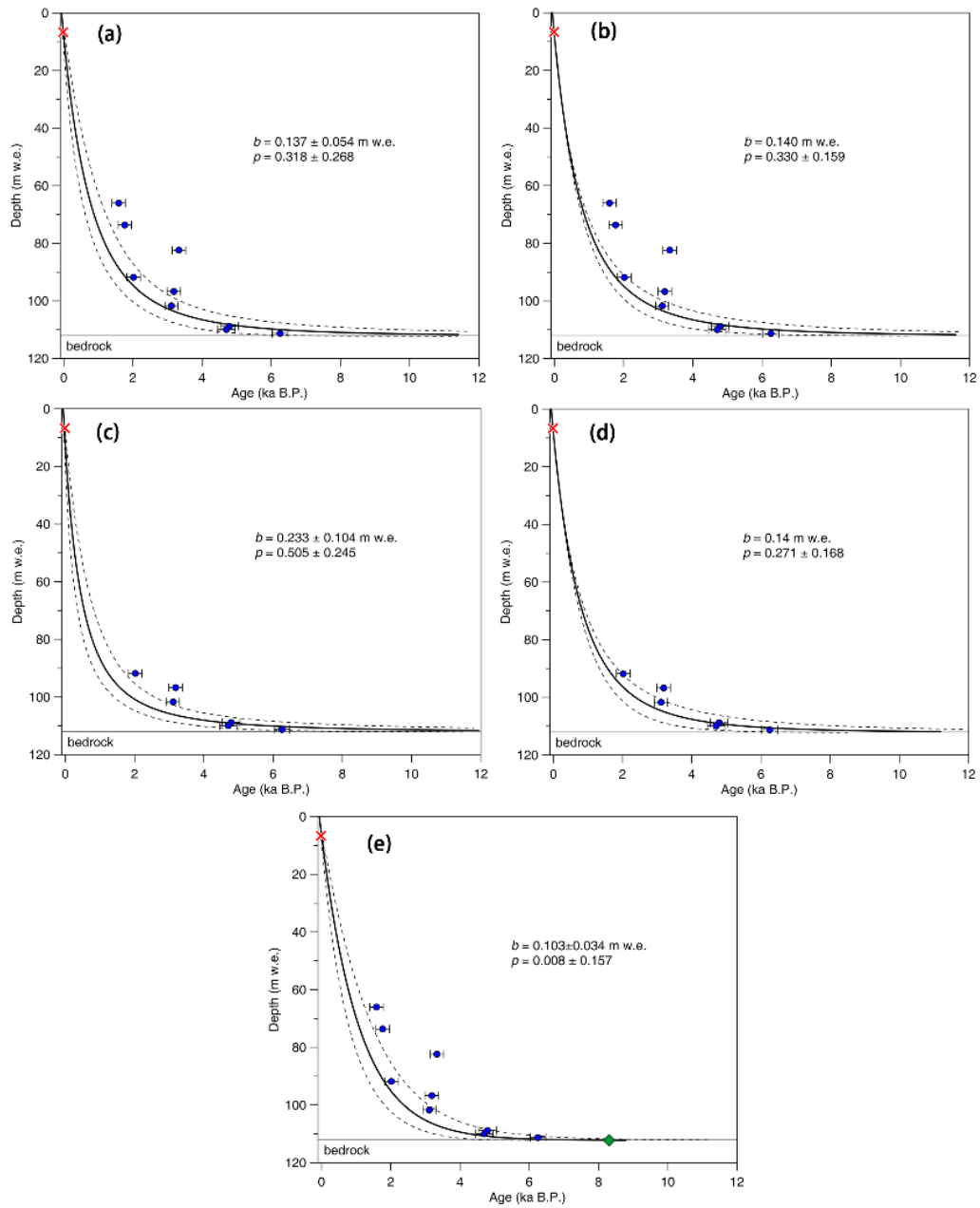


Figure S7. The depth-age relationship of the Chongce Core 2 based on the two-parameter model.

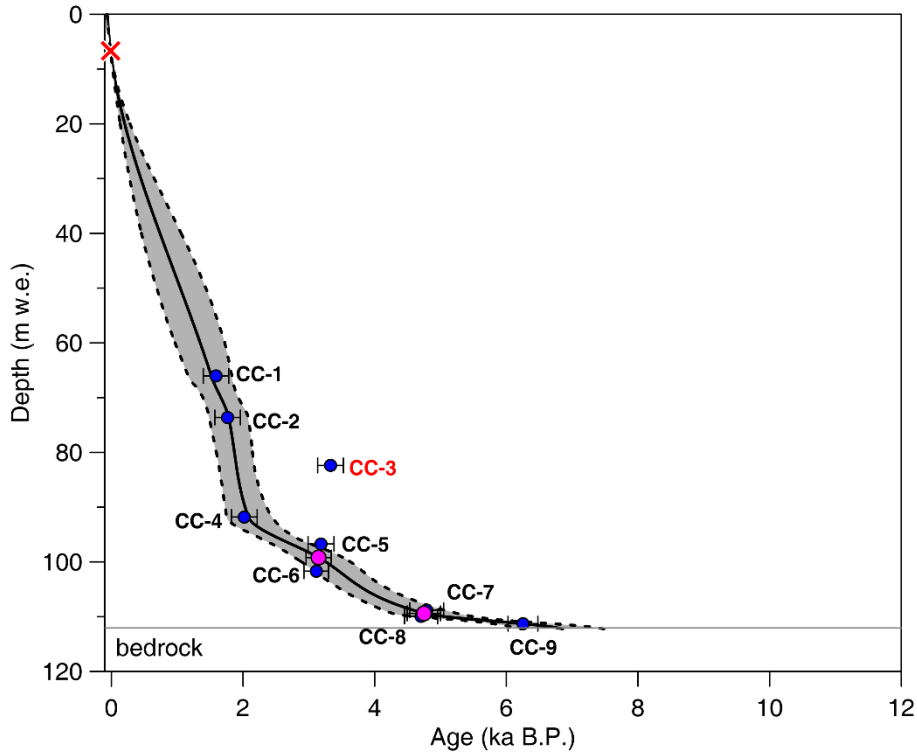


Figure S8. The age-depth relationship for the Chongce Core 2 based on 2000 Monte Carlo simulations fitting the absolute dated age horizons. Solid black lines indicate the mean values, and dotted lines indicate the 1σ confidence interval. The red cross stands for the reference layer of the β activity peak in 1963 A.D. (An et al., 2016). Blue circle show the individual calibrated WIOC ^{14}C ages, and the magenta dots represent the average of the CC-5 and CC-6, and the average of CC-7 and CC-8 ages at their average depths. Error bars represents the 1σ uncertainty. Note that the two magenta dots are included in the Monte Carlo simulation instead of the four original data points because the slight age reversals, but all the CC-5, CC-6, CC-7, and CC-8 are located within 1σ uncertainty range. In addition, CC-3 (non-tractable reversal) is regarded as an outlier and not included in the simulations, because its lower 2σ margin falls outside the upper 2σ margin of the subsequent point in the dating table.

Table S1. Details of ice samples for β -activity measurements.

Sample #	Depth (m)	Depth (m w.e.)	Length (m)	Length (m w.e.)	β activity (dph kg^{-1})
1	0.000-0.710	0.000-0.406	0.710	0.406	555.1
2	0.710-1.150	0.406-0.771	0.440	0.365	936.5
3	1.150-1.720	0.771-1.253	0.570	0.482	597.9
4	1.720-2.185	1.253-1.648	0.465	0.395	499.2
5	2.185-2.575	1.648-1.981	0.390	0.333	505.6
6	2.575-2.945	1.981-2.297	0.370	0.316	539.1
7	2.945-3.355	2.297-2.648	0.410	0.351	416.7

8	3.355-3.890	2.648-3.110	0.535	0.462	518.4
9	3.890-4.350	3.110-3.504	0.460	0.393	396.1
10	4.350-4.805	3.504-3.889	0.455	0.385	439.4
11	4.805-5.270	3.889-4.288	0.465	0.399	1754.5
12	5.270-5.780	4.288-4.735	0.510	0.447	385.8
13	5.780-6.320	4.735-5.198	0.540	0.463	504.9
14	6.320-6.780	5.198-5.593	0.460	0.395	749.1
15	6.780-7.200	5.593-5.948	0.420	0.355	963.2
16	7.200-7.690	5.948-6.362	0.490	0.414	224.9
17	7.690-8.170	6.362-6.767	0.480	0.406	1709.9
18	8.170-8.630	6.767-7.158	0.460	0.390	1910.3
19	8.630-9.120	7.158-7.571	0.490	0.413	479.9
20	9.120-9.580	7.571-7.977	0.460	0.407	574.2
21	9.580-10.020	7.977-8.361	0.440	0.384	98.6
22	10.020-10.550	8.361-8.819	0.530	0.457	682.8
23	10.550-11.060	8.819-9.254	0.510	0.435	262.6
24	11.060-11.490	9.254-9.618	0.430	0.364	503.8
25	11.490-12.015	9.618-10.061	0.525	0.444	705.8
26	12.015-12.525	10.061-10.494	0.510	0.433	168.7
27	12.525-12.925	10.494-10.833	0.400	0.339	282.9
28	12.925-13.375	10.833-11.203	0.450	0.370	191.8
29	13.375-13.845	11.203-11.608	0.470	0.405	673.8
30	13.845-14.305	11.608-11.999	0.460	0.392	269.3
31	14.305-14.805	11.999-12.410	0.500	0.411	324.3

100 **Table S2.** Results of radiocarbon measurements for the Chongce 135.81 m Core 2 ice core samples. For the calibrated calendar year, ranges are given with 68.2% probability.

Sample #	Depth (m)	Depth (m w.e.)	Mass (g)	WIOC (μg)	F ¹⁴ C	¹⁴ C age (ka B.P.) ^a	calibrated age (ka B.P.) ^b
CC-1	79.46-80.21	65.74-66.31	307.7	20.31 ± 1.22	0.81 ± 0.01	1.679 ± 0.078	1.445-1.704
CC-2	88.82-89.56	73.31-73.92	302.9	24.26 ± 1.41	0.80 ± 0.01	1.831 ± 0.138	1.572-1.921
CC-3	99.44-100.10	82.12-82.65	304.6	13.79 ± 0.89	0.68 ± 0.01	3.133 ± 0.161	3.157-3.560
CC-4	110.58-111.35	91.48-92.10	342.6	24.88 ± 1.44	0.78 ± 0.01	2.037 ± 0.142	1.827-2.296
CC-5	116.62-117.43	96.39-97.05	330.9	9.09 ± 0.65	0.69 ± 0.01	3.012 ± 0.164	2.978-3.377
CC-6	122.64-123.36	101.40-101.98	338.6	17.60 ± 1.08	0.69 ± 0.01	2.944 ± 0.157	2.892-3.331
CC-7	131.41-132.10	108.54-109.12	324.6	22.64 ± 1.33	0.59 ± 0.01	4.228 ± 0.176	4.451-5.036
CC-8	132.65-133.51	109.59-110.31	392.7	23.55 ± 1.38	0.60 ± 0.01	4.169 ± 0.175	4.424-4.951
CC-9	134.31-135.03	110.98-111.59	292.4	22.98 ± 1.35	0.51 ± 0.01	5.466 ± 0.201	5.997-6.443

^a“¹⁴C age” denotes conventional radiocarbon age, which is calculated from the formula: $t = -8033 \times \ln(F_s)$, where t is conventional radiocarbon age, F_s is the ¹⁴C / ¹²C ratio of the sample divided by the same ratio of the modern standard.

105 ^b“calibrated age” denotes the calibrated age using OxCal v4.4 online program (Ramsey and Lee, 2013)

with the Northern (IntCal13) calibration curve (Reimer et al., 2013).